Electronic Supplementary Material (ESI) for Journal of Materials Chemistry C.

Supplementary Information

Electrical and electrochemical characterization of proton transfer at the interface between chitosan and PdHx

J.T. Robinson†[1], J.J. Pietron †[1], B. Blue[2], F.K. Perkins[1], E. Josberger[3,4], Y. Deng[3], M. Rolandi[4,5]

[1]*Naval Research Laboratory, Washington, District of Columbia 20375*
[2]*University of Central Florida, Orlando FL 32816*
[3]*University of Washington, Department of Materials Science and Engineering, Seattle, Washington 98195*
[4]*University of Washington, Department of Materials Science and Engineering, Seattle, Washington 98195*
[5]*University of California, Santa Cruz, Dept. of Electrical Engineering, CA, 95064.*

†Equal Contribution

1. Device Fabrication: Figure S1A highlights the two lithographic approaches considered. In the first approach, the chitosan film is deposited and etched (in O2 Plasma) before metallization, where in the second approach, the chitosan film is deposited and etched after metallization. The two primary drawbacks to the first approach are the fact that: (i) several chemical treatments (resists and solvents) are used in between the formation of the chitosan/metal interface and (ii) during device operation under humid environments, the chitosan film swells and contracts depending on the relative humidity. When the metal layer contacts chitosan from the top (1st approach), the metal experiences stress as the underlying chitosan expands and contracts, and thereby changes the nature of the contact interface. In the remainder of the work described here, we only discuss devices fabricated using the second approach (i.e., chitosan on top of the electrode).

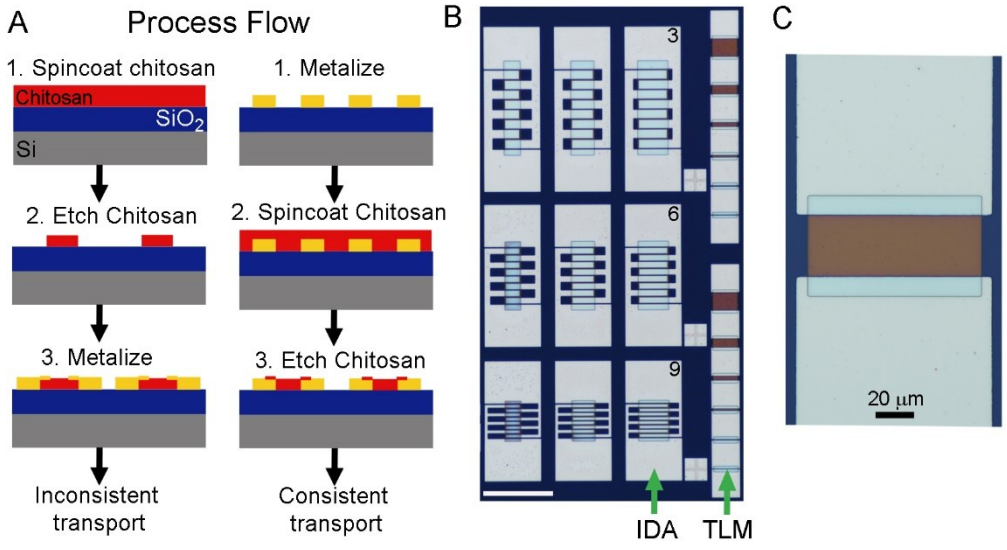

Figure S1. Lithographically-defined, two-terminal devices for measuring conductivity and the electrochemical response of chitosan films. (A) Chitosan devices were fabricated using two different processing flows, which result in different reliabilities of the devices as labeled. (B) Optical micrograph showing the two device structures used in this study: (i) interdigitated arrays (IDA) and (ii) transmission line measurements (TLM) (scale bar = 250 um). (C) Zoom-in showing one TLM device.

2. Control measurements without chitosan films: To rule out the possibility of electronic conduction across a water film alone on the SiO_2 surface, I–V measurements were performed on 2 μm wide TLM devices without chitosan. For V_{DS} sweeps between 0 to 1V, the chitosan-free devices produced noise limited current data on the order of pA, both in the presence and absence of hydrogen in 75% RH (data not shown). This experiment indicates that surface conduction does not contribute to the measured electronic signal.

3. Calculation of proton concentration in chitosan solutions: a 2:1 (vol:vol) mixture of water and glacial acetic acid yields a concentration of ~5.6 M acetic acid. This number derives from an approximate simple weak acid calculation.

The density of glacial acetic acid is 1.049 g/cm^3. In a 2:1 mixture of water and acetic acid, neglecting volume changes for mixing, one has ~334 g acetic acid/liter of solution. The molecular weight of acetic acid is 60.05 g/mole, yielding a solution of 334 g/(60.05 g/mol) = 5.6 M.

The K_A (acid dissociation constant) for acetic acid is 1.8×10^{-5}; when one solves the quadratic equation for the weak acid dissociation: $HA = H^+ + A^-$; setting the concentration of HA (acetic acid) = 5.5M –x , where x is the concentration of dissociated acetic acid, and the concentrations of dissociated protons (H^+) and acetate ion (A^-) are both equal to x, the equilibrium equation is:

$x^2/[5.5 - x] = 1.8 \times 10^{-5}$

Solving the quadratic yields $x = 1 \times 10^{-3}$, or about 1 mM.

The concentration of H_2 is approximated from the equilibrium concentration of saturated water at 1 atm H_2 pressure, which is 7.14×10^{-3} M; assuming that Henry's law is obeyed and the concentration of H_2 in the solution is a linear function of the H_2 pressure over the solution, at 5% atmospheric pressure of H_2, C $[H_2] = 3.6 \times 10^{-4}$ M

By the Nernst equation, solved for the H_2/H^+ electrochemical couple: $E - E^0 = 0.059$ mV * log $[H^+]/[H_2]$, where $E^0 = 0$ V; the relative concentrations of H^+ and H_2 result in a potential of +2.6 mV (0.0026 V) from the equilibrium potential of H^+ and H_2, which is 0.0 V; for simplicity we treat the films as if they are effectively poised at 0 V.

4. Estimation of electrochemical reference and reaction potentials in the chitosan films

The cathode (the electrode held at 0 V in the experiments here) serves as a reversible hydrogen electrode (RHE), the potential of which is determined by Eq. 2. The value of 0 V versus RHE is defined as the potential in which the reaction in Eq. 2 yields zero current at the values of $[H^+]$ of $[H_2]$ in the environment around the cathode. Although the pH in the films is also hard to know exactly (see the section below), as the films derive from a chitosan in a concentrated acetic acid solution (~5.6 M) estimated to yield ~1 mM acid,

which is subsequently spun down to form the films, which are subsequently hydrated, The reference potential of the NHE is defined as 0 V under "standard" electrochemical conditions ($[H^+]$ = 1 M; $[H_2]$ = 1 atm) by Eq. 2.

The standard reported equilibrium potential ($E^{0'}$) values for electrochemical reactions are those occurring under those same standard conditions. The $E^{0'}$ values of all electrochemical reactions in which involve exchange of equal numbers of protons and electrons (including Eqs. 1 and 2 in the main text and several reactions named subsequently) will shift by approximately the same amount as the reference potential, making the use of the known $E^{0'}$values for the reactions versus the NHE reasonable estimates for the E^0 occurring *in situ* versus the RHE.

5. Digital simulation of electrochemical I–V data in linear sweep voltammetry

Even in the simplest case, where the electrochemical reactions are diffusion controlled (i.e. have immeasurably fast kinetics), numerical solutions are required to describe the time-varying currents. The current is described by Fick's first (Eq. S1) law of diffusion at a given point in time and Fick's second law (Eq. S2) in the more general time-varying case.[i]

$$i = nFAD(\delta C/\delta x) \qquad \text{(S1)}$$

$$\delta C(x,t)/\delta t = D[\delta^2 C(x,t)/\delta x^2] \qquad \text{(S2)}$$

In Eqs. S1 and S2, n is the number of electrons transferred in a Faradaic reaction, A is the electrode area, F is Faraday's constant (~96,500 Coulombs/mole electrons), D is the diffusion coefficient, and $\delta C/\delta x$ is the concentration gradient of the electroactive species near the electrode surface at a given point in time, and $\delta C(x,t)/\delta t$ is the time-varying concentration gradient at the electrode surface. The situation becomes even more complicated when electron transfer kinetics factor substantially into the currents, the electron transfer rate constants, k (potential-dependent) and k^0 (the rate constant at $E^{0'}$, also known as the standard rate constant), factors into the solution as described in Eqs. S3 and S4. The variable α is the transfer coefficient, which is usually taken to be ½ in symmetrical electrochemical reactions (where the rate constants for the forward and back reactions are similar).[i]

$$i = nFAD\, k\, \delta C(x,t)/\delta t \qquad \text{(S3)}$$

$$k = k^0 \exp(-\alpha nF(E(t)-E^{0'}) \qquad \text{(S4)}$$

Digital simulation breaks the time-varying diffusion gradient problem into discrete space and time elements that are allowed to iteratively evolve.[ii] The variables that we can input into the simulation are n, A, D, and C_R and C_O , or the bulk concentration of electroactive species in both the reduced and oxidized forms (before the electrode is "turned on" and the experiment is started, and k^0. The cell resistance, R, is also input into the simulation (not shown in the analytical expressions). After making reasonable initial

assumptions for these variables, values of k^0 and R are varied until best fits of the simulated data to the experimental data are achieved.

6. Assumptions made for proton [H^+] and hydrogen [H_2] concentrations, electrode areas, and diffusion coefficient values in the digital simulations of I–V curves

The value of A used for the TLM devices was the product of the width of the chitosan films on the electrode pairs (~100 µm or 1×10^{-2} cm) and the length of the overlapping "lip" of the chitosan films on the electrodes (Fig. S1c; ~10 µm or 1×10^{-3} cm), which was 1×10^{-5} cm^2. At the interdigitated array electrodes, the dimensions of the top of one set of the drain electrodes (10 µm x 105 µm) was multiplied by 5 (there are 5 pairs including the part of the contact pad in contact with the chitosan film which also features a ~10 µm overlap) to yield a total area of 7.25×10^{-5} cm^2.

The value of n (the number of electrons transferred in the hydrogen oxidation reaction, and its reverse reaction, the hydrogen evolution reaction (HOR and HER) were set at 2.

As described in section 3 above, the proton concentration in the chitosan solutions from which the films were derived was ~1 mM. This value may change in an unknowable way during the process of spin-coating the solutions into films. The proton concentration can in principle go up or down, as the effects of (1) decreasing the volume of solvent and (2) evaporation of acetic acid oppose one another, the dominance of which will depend on the water retention of the films. Water retention in the films is also likely to differ between high molecular weight and low molecular weight chitosan-derived films.

We fixed the diffusion coefficient, D, to 2×10^{-6} cm^2 s^{-1}, a value similar to those reported for small molecules in 5 weight% chitosan gels.[iii] We elected to use the same diffusion coefficient across all films. This is very clearly an approximation, as the actual value of D will depend on the conditions in the film itself, particularly on water content. In reality, the currents observed will be a convolution of the resultant concentrations and diffusion coefficients of both protons and H_2 molecules in a given film.

We chose to adjust the values of proton concentration in the digital simulations of the I–V curves to values that enabled other variables to easily converge across measurements made at a given film cast on a given device set, while keeping D constant, as described above. We also simply used C [H_2] = 3.6×10^{-4} M, the value linearly extrapolated from the saturation value of 5% H_2 in water at 1 atm pressure of the gas mixture.

Specific values used for [H^+]:

Chitosan films at TLM devices (Simulations in Fig 3): 1.2 mM
High MW chitosan films at TLM devices (Simulations in Fig S3): 26.6 mM
Chitosan films at IDA devices (Simulations in Fig 4): 7.0 mM

7. Analytical descriptions of feedback and classical diffusion-controlled electrochemistry at IDA devices:

The steady-state current response for kinetically fast electrochemical reactions at IDA devices is:

$$I_{lim} = mbnFC^{*}D[0.637 \ln[2.55 [1 + w_a/w_g]] - 0.19/ (1 + w_a/w_g)^2] \quad (S5)^{iv}$$

In Eq. S5, *m* is the total number of anode/cathode (or source-drain) pairs; *b* is the length of the individual electrode digits (in this case, approximated as the width of the chitosan film covering the digits); *n* is the number of electrons transferred per molecule in the electrochemical reaction; C^{*} is the concentration of the electroactive species (in this case the concentration of H_2 dissolved in the chitosan films); w_a is the width of the anode; and w_g is the inter-electrode gap. From Eqn. 9 we calculated the current responses for IDA devices 3, 6, and 9 at a full steady-state response to be 77.6 nA, 68.3 nA, and 53.9 nA, respectively (using n = 2 for the electrochemical HOR (reverse of Eq. 2) and the same values of C^{*} and D used in the digital simulation of the LSV used in Fig. 3 and 4).

Although the chitosan films are not adequately thick to establish the hemispherical diffusion geometry from each of the electrode digits to establish a steady-state feedback loop, feedback between the anode and cathode electrode arrays is probable on the time scale of the experiments. Because the inter-electrode gaps are 5 µm each, the duration of experiment, defined by the length of the voltammetric scans need only be long enough for H_2 to diffuse 5 µm within the film to achieve some degree of feedback between electrode edges; electrode center-to-center feedback only requires 5 µm + the width of one digit width (i.e., half a digit length at each digit + width of the gap + an additional half digit width to the center of the adjacent digit) to generate cross talk through the entire diffusion profiles. Using the estimated diffusion coefficients of ~2×10^{-6} cm^2 s^{-1} (the same as was used for the chitosan TLM devices) for H_2 in chitosan films, the estimated diffusion distances of H_2 in the chitosan films, using Einstein's well-known diffusion relation (Eq. S6) are given in Table 2:

$$\text{Diffusion distance} = x = (Dt)^{1/2} \quad (S6)$$

Where D is the diffusion coefficient of the molecule in the medium and t is the time of the diffusion process.

Table 1. Duration of the voltammetric scans at chitosan films deposited on IDA device 9

Scan Rate (mV s^{-1})	Time of voltammetric sweep (s)	Diffusion distance (µm) $x = (Dt)^{1/2}$
19.3	51.8	101
43	23.3	68
110	9.1	42
290	3.4	26
580	1.7	18.4

At all scan rates and at all IDA geometries used, the experiment is sufficiently long to allow edge-to-edge diffusion of the electrochemical products at both the anode and cathode electrode arrays, and center-to-center diffusion is possible at IDA devices 6 and 9 (with center-to-center distances of 15 and 25 µm, respectively) at all scan rates. At IDA device 3, with a center-to-center distance of 35 um, center-to-center diffusion can occur at all but the two highest scan rates. Thus, some degree of electrochemical feedback (and thus faradaic current enhancement) is expected in all cases—just not sufficient feedback to generate the currents predicted by Eq. 2.

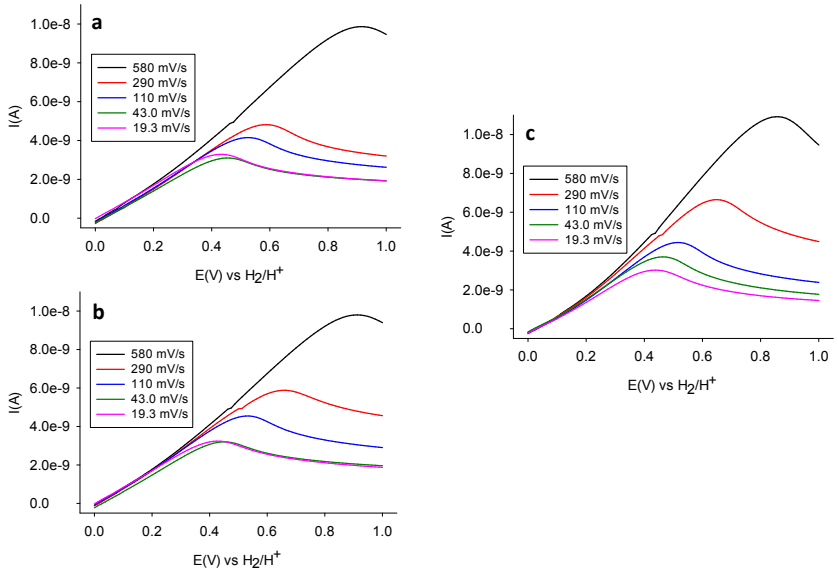

Figure S2 Current–voltage data taken with chitosan films deposited on IDA devices from Figure S1B: (a) #3, (b) #6, and (c) #9, each at voltage scan rates of 19.3, 43.0, 110, 290, and 580 mV s^{-1} (RH=75%, H2=5%).

8. Essential features of complex plane impedance plots: The x-axis values represent the vector component of the measured current that are in-phase with the voltage perturbation (the so-called "real" component of the current and impedance), whereas the y-axis values represent the component of current (and thus impedance) that is 90 ° out of phase with the voltage perturbation (the so-called "imaginary" component of the current and impedance). The real component of the impedance represents the resistive component of the medium, whereas the imaginary impedance corresponds to a capacitive element.[v]

9. 'High' molecular weight (MW=600-900kD) chitosan results: As a means to test intrinsic properties of chitosan, we use both 'low' and 'high' MW films. The high MW chitosan devices exhibit I–V curves without obvious peaks (Fig. S3a). The absence is due to the >5× higher currents in the I–V curves for the high MW chitosan TLM devices—the would-be peaks are shifted out of the I–V sweep range by ohmic losses. To establish a quantitative comparison between the low and high MW chitosan films, we fit the experimental I-V data to digitally simulated I–V curves (Fig. S3b–c). As with the low MW chitosan devices, the I–V data at high MW chitosan films are best fit to two separate electrochemical HOR rate constants: one very low—in 10^{-8} cm s^{-1} range—and the other substantially higher at 5×10^{-6} cm s^{-1} (Table S1). The rates are essentially identical to those estimated for the low MW chitosan devices. The resistances associated with the faster HOR pathway, as with the low MW devices, increase monotonically with inter-electrode gap length, and while somewhat smaller (~2×), are essentially similar in value—in the 100's of MΩ range (Table S1). The resistance values that fit best to the kinetically faster HOR kinetics (k_2) at the high MW chitosan are in the low GΩ range. As is the case for the HOR pathway controlled by k_1, the resistances in high MW chitosan are similar to but consistently lower than those estimated for the low MW chitosan films.

The high MW chitosan devices produce larger currents—by about a factor of 5–10—than those observed at the low MW devices. In fitting the data for the high MW chitosan devices, the higher currents were best fit by assuming an approximate 20× higher concentration of protons in the high MW chitosan films than in the films derived from low-MW chitosan. This apparent ability to support higher proton concentrations in high MW chitosan films likely derives from greater water retention by high-MW chitosan: chitosan membranes in general demonstrate lower crystallinity, higher swelling, and higher conductivity with increasing molecular weight of chitosan. The higher currents achievable in the higher MW and concomitantly more water-retaining chitosan films highlights the centrality of the Grothuss water-wire mechanism of proton transport in chitosan-based protonic interfaces.

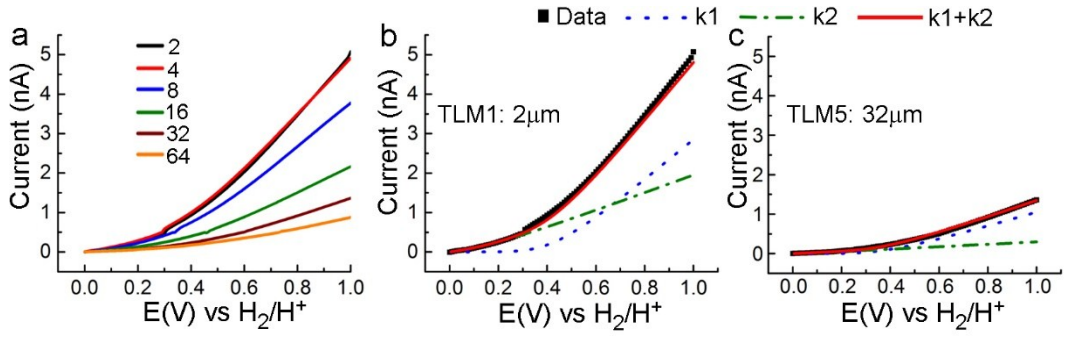

Fig. S3 (a) Experimental I–V data from TLM devices with PdH_x electrodes coated with a high MW chitosan films at 2 to 64-μm channels under 75% RH at 150–mV s^{-1}. (b)–(c) Comparison of experimental (square points) and simulated (lines) I–V data from the high MW chitosan films in (a) at selected electrode pairs with different intervening gap lengths.

Table S1.

Device	Gap (μm)	R_1 (M Ω)	σ(S/cm) (chitosan)	k_1 (cm/s)	R_2 (G Ω)	k_2 (cm/s)	σ (S/cm)
TLM 1	2	160	1.3×10^{-7}	2.0×10^{-8}	0.400	5.0×10^{-6}	5.0×10^{-8}
TLM 2	4	160	2.5×10^{-7}	2.0×10^{-8}	0.400	5.0×10^{-6}	1.0×10^{-7}
TLM 3	8	215	3.7×10^{-7}	2.0×10^{-8}	0.550	5.0×10^{-6}	1.5×10^{-7}
TLM 4	16	350	4.5×10^{-7}	2.0×10^{-8}	1.1	5.0×10^{-6}	1.5×10^{-7}
TLM 5	32	500	6.4×10^{-7}	2.0×10^{-8}	3.0	5.0×10^{-6}	1.1×10^{-7}
TLM 6	64	800	8.0×10^{-7}	2.0×10^{-8}	5.0	5.0×10^{-6}	1.3×10^{-7}

Interelectrode resistances (R) and electrochemical hydrogen oxidation reaction rate constants (k) estimated from digital simulation of I–V curves measured using PdH_x electrodes under 75% RH at TLM devices coated with high MW chitosan films.

[i] Bard, A. J.; Faulkner, L. R., *Electrochemical Methods: Fundamentals and Applications*; Wiley, 2000.

[ii] Feldberg, S. Digital Simulation: a General Method for Solving Electrochemical Diffusion–Kinetic Problems, in A. J. Bard (Ed.), *Electroanalytical Chemistry, Vol. 3,* Marcel Dekker, New York, 1969, pp 199–295

[iii] C. García-Aparicio, I. Quijada-Garrido, L. Garrido, *J. Coll. Interfac. Sci.* **2012,** *368,* 14–29

[iv] Aoki, K.; Morita, M.; Niwa, O.; Tabei, H., Quantitative Analysis of Reversible Diffusion-Controlled Currents of Redox Soluble Species at Interdigitated Array Electrodes under Steady-State Conditions. *Journal of Electroanalytical Chemistry and Interfacial Electrochemistry* **1988**, *256*, 269-282.

[v] Huggins, R. A., Simple Method to Determine Electronic and Ionic Components of the Conductivity in Mixed Conductors a Review. *Ionics* **2002**, *8*, 300-313.